Available online at www.sciencedirect.com
SCIENCE DIRECT®
International Journal of Solids and Structures 43 (2006) 5525–5540
INTERNATIONAL JOURNAL OF SOLIDS and STRUCTURES
www.elsevier.com/locate/ijsolstr

Natural frequencies and mode shapes for axisymmetric vibrations of shells in turning-point range

Zhi-Liang Zhang [a,b], Chang-Jun Cheng [a,*]

[a] Department of Mechanics, Shanghai Institute of Applied Mathematics and Mechanics, Shanghai University, Shanghai 200072, China
[b] Department of Physics, Institute of Applied Acoustics, Zhejiang Normal University, Jinhua Zhejiang 321004, China

Received 30 April 2005; received in revised form 29 June 2005
Available online 30 August 2005

Abstract

In the present paper, the natural frequencies and modes in turning-point frequency range where the governing equations have turning points are studied for revolution shells under various boundary conditions by applying the uniformly valid solutions obtained in a previous paper. Due to the presence of the turning points in this frequency range, several novel features emerge from the analytic and computational results for vibration of shells, in which the most basic nature is the coupling of bending and membrane solutions for frequencies and modes. And simple expressions for the bending-edge-condition effect and frequency spacing are presented.

Keywords: Natural frequencies and modes; Turning-point range; Revolution shell; Novel feature

1. Introduction

In revolution shell vibrations, when the frequency parameter Ω lies within the frequency range

$$\min[R_2^{-1}(s)] \leqslant \Omega \leqslant \max[R_2^{-1}(s)] \quad (a \leqslant s \leqslant b), \tag{1}$$

there exist turning points where $\Omega R_2 = 1$ in governing equations and in shells. The frequency range given by (1) is called the turning-point range or the transitional range. Ross (1966), Steele (1976), Gol'denveizer et al. (1979), Gol'denveizer (1980), Zhang (1988), Zhang and Zhang (1991) and other researchers have investigated the vibration of shells in this range with asymptotic methods. In a previous paper the authors Zhang

* Corresponding author. Tel./fax: +86 21 56380560.
E-mail addresses: zzl@zjnu.cn (Z.-L. Zhang), chjcheng@staff.shu.edu.cn (C.-J. Cheng).

0020-7683/$ - see front matter © 2005 Elsevier Ltd. All rights reserved.
doi:10.1016/j.ijsolstr.2005.06.082

Notation

All the quantities are dimensionless except the characteristic shell radius R^*, Young's modulus E, the mass density ρ, the angular frequency ω and all the quantities with superscripts *.

$B = B^*/R^*$ Lame's coefficient of the second principal coordinate
$b_2(s) = \Omega^2 - R_2^{-2}(s)$ coefficient of the second-order derivative of membrane system
$h = h^*/R^*$ thickness of shell
$M_1, M_2 = M_1^*, M_2^*/(Eh^*R^*\varepsilon^4)$ moments
$N_1, N_2 = N_1^*, N_2^*(1-\nu^2)/(Eh^*)$ membrane stress resultants
$Q_1 = Q_1^*/(Eh^*\varepsilon^4)$ shear stress resultant
$R_1 = R_1^*/R^*, R_2 = R_2^*/R^*$ principal radii of curvature
$s = s^*/R^*$ first principal coordinate along longitude
$s = a$, b two ends of truncated shell and $b_2(a) < 0$ and $b_2(b) > 0$
s_* location of the turning point and $b_2(s_*) = 0$
$u = u^*/R^*, w = w^*/R^*$ tangential and normal displacements
$z(s) = \left(\frac{5}{4}\int_{s_*}^{s} b_2^{1/4}(x)\,\mathrm{d}x\right)^{4/5}$ Langer's variable
$\beta = u/R_1 - w'$ rotation
$\varepsilon^4 = \mu^5 = h^2/12/(1-\nu^2)$ parameter of shell thickness
$\zeta = z/\mu$ stretching independent variable
ν Poisson's ratio, $\nu = 0.3$ in calculation
$\Omega^2 = \rho\omega^2 R^{*2}/E$ frequency parameter

Subscripts
1 and 2 first and second principal coordinates

and Cheng (submitted for publication) improved the existing work and obtained the uniformly valid solutions in quite good agreement with numerical calculations. The obtained uniformly valid solutions exhibit a novel feature: a symmetric coupling structure in connection of solutions on two sides of the turning point, namely, a membrane solution on one side of the turning point is connected to a bending solution as well as itself on the other side; at the same time a bending solution is connected to a membrane solution beside itself (see Eq. (10)). And as will be seen, it is due to the coupling symmetry of the solutions that correct results would be led to in application of these solutions.

We shall restrict ourselves to dealing with axisymmetric vibration of truncated revolution shells with only one first-order turning point for any given frequency within the range (1), which implies that the shell is not locally cylindrical or spherical at any point of the generatrix of shells and that R_2 is a monotone function for s. Even for the conical shells, the simplest structure up to the restriction, while the natural frequencies and modes have been studied by many investigators, e.g., Tang (1964), Seide (1965), Hartung and Loden (1970), Frankort (1975), Sun (1987) and Tao and Zhang (1998), there are few analytic results for the frequencies and especially for the modes in this frequency range. The purpose of the present paper is to use the results obtained by Zhang and Cheng (submitted for publication) to determine the natural frequencies and mode shapes for various boundary conditions and to clarify the basic nature of vibration of revolution shells in the turning-point range. Analysis and computation show that the results given by the present paper agree well with those obtained from the finite element method and those of Hartung and Loden (1970) and Frankort (1975), which are mostly based on numerical calculation in the turning-point range.

The presence of turning points makes the vibration of shells in the turning-point range greatly different from that in other frequency range. After examination of some 3000 different configurations, Hartung and Loden (1970) observed: "it is in regime II (turning-point range) that the novel feature of the modal behavior of the cone is exhibited". Further, the problem under present study has extensive application background in engineering: for example, the turning-point range is a crucial frequency interval for loudspeakers and the characteristic frequencies are of high interest in design of loudspeakers.

2. Formulation

For convenient read, in this section we shall rewrite the main results given by Zhang and Cheng (submitted for publication). Let the value of the analytic membrane solution at the turning-point $u_{6(0)}$ be

$$u_{6(0)} \equiv u_6(s_*) = \varepsilon^{\frac{1}{2}}[R_1^{-1}(s_*) + \nu R_2^{-1}(s_*)]z'(s_*)^{-1}. \tag{2}$$

Except the analytic membrane solution which is almost unaffected by the presence of the turning point, the remaining five solutions can be rewritten in terms of the so-called generalized related functions $Z_h(\zeta,p)$ and $R(\zeta,p)$ as

$$\begin{aligned}
&u_h = \mu\alpha_1 Z_h(\zeta,1),\\
&w_h = \gamma_0 Z_h(\zeta,0)\ (h=1,2,3),\\
&u_4 = \mu\alpha_1\zeta^{-1}Z_4(\zeta,-3) - u_6\zeta^{-1}Z_4(\zeta,2),\\
&w_4 = \gamma_0 Z_4(\zeta,0) - w_6 Z_4(\zeta,1),\\
&u_5 = u_{5m} - u_6[\zeta^{-1}R(\zeta,2) + \ln|\zeta| + \gamma - 1] + \mu\alpha_1\zeta^{-1}R(\zeta,-3),\\
&w_5 = w_{5m} - w_6[R(\zeta,1) + \ln|\zeta| + \gamma] + \gamma_0\zeta^{-1}R(\zeta,-4),
\end{aligned} \tag{3}$$

where $\gamma = 0.5772156649\ldots$ is Euler's constant, u_{5m}, w_{5m} and u_6, w_6 are respectively the singular and analytic solutions of the membrane system obtained by setting $\varepsilon = 0$ in the parent system, which in the turning-point range usually have to be found by numerical integration on the second-order membrane equations or in series form, and

$$\begin{aligned}
\alpha_1 &= -\mu^{-3/8}\left(\frac{1}{R_1} + \frac{\nu}{R_2}\right)\left(\frac{B(s_*)}{B(s)}\right)^{1/2}\left(\frac{z'(s_*)}{z'(s)}\right)^{5/2},\\
\gamma_0 &= \mu^{-3/8}z'(s_*)\left(\frac{B(s_*)}{B(s)}\right)^{1/2}\left(\frac{z'(s_*)}{z'(s)}\right)^{3/2}.
\end{aligned} \tag{4}$$

The solutions are all analytic and uniformly valid. In the turning-point region the following power series representations of the generalized related functions will be used:

$$\begin{bmatrix} R(\zeta,p)\\ Z_1(\zeta,p)\\ Z_2(\zeta,p)\\ Z_3(\zeta,p)\\ Z_4(\zeta,p)\end{bmatrix} = \frac{5^{-\frac{p+4}{5}}}{\pi}\sum_0^\infty \frac{5^{n/5}\zeta^n}{n!}\Gamma^*\left(\frac{n+1-p}{5}\right)\begin{bmatrix} \pi\cos(n+1-p)\alpha\\ \sin 2(n+1-p)\alpha - 0.2J(\zeta,p)\\ \cos(n+1-p)\alpha - \cos 2(n+1-p)\alpha\\ 1-\cos(n+1-p)\alpha\\ \sin(n+1-p)\alpha + 0.4J(\zeta,p)\end{bmatrix}, \tag{5}$$

where

$$\begin{aligned}
&\Gamma^*(x)|_{x\neq 0,-1,-2,\ldots} = \Gamma(x), \quad \Gamma^*(0) = \ln 5 - \gamma,\\
&J(\zeta,p) = 0 (p \leqslant 0), \quad J(\zeta,1) = 1, J(\zeta,2) = \zeta.
\end{aligned}$$

And outside the turning-point region ($|\zeta| > 5$), the following asymptotical representations are then applicable:

$$\begin{aligned}
&\begin{bmatrix} Z_1(\zeta,p) \\ Z_2(\zeta,p) \\ Z_3(\zeta,p) \\ Z_4(\zeta,p) \end{bmatrix} \sim \frac{\zeta^{-\frac{2p+3}{8}}}{\sqrt{2\pi}} \begin{bmatrix} (-1)^p \exp(-\theta) \\ \cos[\theta-(2p-1)\pi/4] \\ \exp(\theta) \\ \sin[\theta-(2p-1)\pi/4]+J(\zeta,p) \end{bmatrix} \text{ as } \zeta \to +\infty, \\
&\theta = \frac{4}{5}\zeta^{4/5} = \frac{1}{\varepsilon}\int_{s_*}^{s} b_2^{1/4}(x)\,\mathrm{d}x = \theta(s); \\
&\begin{bmatrix} Z_1(\zeta,p) \\ Z_2(\zeta,p) \\ Z_3(\zeta,p) \\ Z_4(\zeta,p) \end{bmatrix} \sim \frac{|\zeta|^{-\frac{2p+3}{8}}}{\sqrt{2\pi}} \begin{bmatrix} \exp(\eta)\sin[\eta+(6p+1)\pi/8] \\ \exp(\eta)\cos[\eta+(6p+1)\pi/8] \\ \exp(-\eta)\cos[\eta+(2p+3)\pi/8] \\ \exp(-\eta)\sin[\eta+(2p+3)\pi/8] \end{bmatrix} \text{ as } \zeta \to -\infty, \\
&\eta = \frac{4}{5\sqrt{2}}|\zeta|^{4/5} = \frac{1}{\sqrt{2}\varepsilon}\int_{s}^{s_*} [-b(x)]^{1/4}\,\mathrm{d}x = \eta(s)
\end{aligned} \tag{6}$$

and

$$\begin{aligned}
&R(\zeta,p) \equiv R_m \sim \begin{cases} (-p)!(-\zeta)^{p-1} & (p \leqslant 0) \\ -\ln|\zeta| - \gamma & (p=1) \\ -\zeta(\ln|\zeta| + \gamma - 1) & (p=2) \end{cases} \quad \text{as } \zeta \to -\infty; \\
&R(\zeta,p) \sim R_m + \pi Z_2(\zeta,p) \text{ as } \zeta \to +\infty.
\end{aligned} \tag{7}$$

Physically, the interest quantities are given by

$$\begin{aligned}
&N_{1h} = C_N Z_h(\zeta,1)\ (h=1,2,3), \\
&N_{14} = C_N\zeta^{-1}Z_4(\zeta,-3) - N_{16}\zeta^{-1}Z_4(\zeta,2), \\
&\beta_h = -\mu^{-1}z'\gamma_0 Z_h(\zeta,-1), \\
&M_{1h} = -\mu^{-2}z'^2\gamma_0 Z_h(\zeta,-2), \\
&Q_{1h} = -\mu^{-3}z'^3\gamma_0 Z_h(\zeta,-3),\ (h=1,2,3,4), \\
&N_{15} = N_{15m} - N_{16}[\zeta^{-1}R(\zeta,2) + \ln\zeta + \gamma - 1] + C_N\zeta^{-1}R(\zeta,-3), \\
&\beta_5 = -\mu^{-1}z'\gamma_0 R(\zeta,-1), \\
&M_{15} = -\mu^{-2}z'^2\gamma_0 R(\zeta,-2), \\
&Q_{15} = -\mu^{-3}z'^3\gamma_0 R(\zeta,-3),
\end{aligned} \tag{8}$$

where

$$C_N = -(1-v^2)\mu\alpha_1\frac{B'}{B}\left(v+\frac{R_2}{R_1}\right)^{-1}, \quad N_{15m} = (1-v^2)\left(v+\frac{R_2}{R_1}\right)^{-1}\left(b_2R_2w_{5m} - \frac{B'}{B}u_{5m}\right).$$

3. Frequency and mode for truncated revolution shells

The general solutions of axisymmetric vibration of revolution shells can be written in the form

$$\begin{aligned}
&u = \sum_{i=0}^{6} A_i u_i, \quad w = \sum_{i=0}^{6} A_i w_i, \quad \beta = \sum_{i=0}^{6} A_i \beta_i, \\
&N = \sum_{i=0}^{6} A_i N_i, \quad M = \sum_{i=0}^{6} A_i M_i, \quad Q = \sum_{i=0}^{6} A_i Q_i,
\end{aligned} \tag{9}$$

where A_i are arbitrary constants, and the subscripts 1 of N_1, M_1 and Q_1 are omitted, without confusion. To see clearly the characteristics of the six solutions, we have to write out the solutions away from the turning-point region obtained by substituting Eqs. (6) and (7) into Eq. (9), namely,

$$
\begin{aligned}
&\text{as } s_* < s \leqslant b:\\
&u = \varepsilon H_u[A_2 s(\theta) + A_3 \mathrm{e}^{\theta}] - A_4[\varepsilon H_u c(\theta) + u_6] + A_5(u_{5m} + \pi\varepsilon H_u s(\theta)) + A_6 u_6,\\
&N = \varepsilon H_n[A_2 s(\theta) + A_3 \mathrm{e}^{\theta}] - A_4[\varepsilon H_n c(\theta) + N_6] + A_5(N_{5m} + \pi\varepsilon H_n s(\theta)) + A_6 N_6,\\
&w = H_w[A_2 c(\theta) + A_3 \mathrm{e}^{\theta}] + A_4[H_w s(\theta) - w_6] + A_5(w_{5m} + \pi H_w c(\theta)) + A_6 w_6,\\
&\beta = -\varepsilon^{-1} b_2^{1/4} H_w[-A_2 s(\theta) + A_3 \mathrm{e}^{\theta} + A_4 c(\theta) - A_5 \pi s(\theta)] + A_6 \beta_6,\\
&M = -\varepsilon^{-2} b_2^{1/2} H_w[-A_2 c(\theta) + A_3 \mathrm{e}^{\theta} - A_4 s(\theta) - A_5 \pi c(\theta)] + A_6 M_6,\\
&Q = -\varepsilon^{-3} b_2^{3/4} H_w[A_2 s(\theta) + A_3 \mathrm{e}^{\theta} - A_4 c(\theta) + A_5 \pi s(\theta)] + A_6 Q_6,\\
&\text{as } a \leqslant s < s_*:\\
&u = -\varepsilon H_u \mathrm{e}^{\eta}[A_1 \sin(\eta - \pi/8) + A_2 \cos(\eta - \pi/8)] + A_5 u_{5m} + A_6 u_6,\\
&N = -\varepsilon H_n \mathrm{e}^{\eta}[A_1 \sin(\eta - \pi/8) + A_2 \cos(\eta - \pi/8)] + A_5 N_{5m} + A_6 N_6,\\
&w = H_w \mathrm{e}^{\eta}[A_1 \sin(\eta + \pi/8) + A_2 \cos(\eta + \pi/8)] + A_5 w_{5m} + A_6 w_6,\\
&\beta = \varepsilon^{-1}|b_2|^{1/4} H_w \mathrm{e}^{\eta}[A_1 \cos(\eta - \pi/8) - A_2 \sin(\eta - \pi/8)] + A_5 \beta_{5m} + A_6 \beta_6,\\
&M = -\varepsilon^{-2}|b_2|^{1/2} H_w \mathrm{e}^{\eta}[A_1 \cos(\eta + \pi/8) - A_2 \sin(\eta + \pi/8)] + A_5 M_{5m} + A_6 M_6,\\
&Q = -\varepsilon^{-3}|b_2|^{3/4} H_w \mathrm{e}^{\eta}[A_1 \sin(\eta - \pi/8) + A_2 \cos(\eta - \pi/8)] + A_5 Q_{5m} + A_6 Q_6,
\end{aligned}
\tag{10}
$$

where θ and η are given by (6), and

$$
\begin{aligned}
&s(\theta) = \sin(\theta + \pi/4), c(\theta) = \cos(\theta + \pi/4),\\
&H_w = \frac{1}{\sqrt{2\pi}} \left(\frac{B(s_*)}{B(s)}\right)^{1/2} \frac{b_2'(s_*)^{3/10}}{|b_2(s)|^{3/8}}, \quad H_u = -\frac{1}{\sqrt{2\pi}} \left(\frac{1}{R_1} + \frac{v}{R_2}\right) \left(\frac{B(s_*)}{B(s)}\right)^{1/2} \frac{b_2'(s_*)^{3/10}}{|b_2(s)|^{5/8}},\\
&H_n = \frac{1 - v^2}{\sqrt{2\pi}} \frac{1}{R_2} \frac{B'(s)}{B(s)} \left(\frac{B(s_*)}{B(s)}\right)^{1/2} \frac{b_2'(s_*)^{3/10}}{|b_2(s)|^{5/8}}.
\end{aligned}
$$

One can see that the first three solutions and the sixth solution are purely of bending and membrane type, respectively, while the fourth and the fifth are of mixed type: in traversing the turning-point region from $s < s_*$ to $s > s_*$ the singular membrane solution (the fifth solution) and the fourth bending solution give birth to the second bending solution and the analytic membrane solution, respectively; and that in the region $a \leqslant s < s_*$ the bending solutions appear only as the boundary layer effect. The above two characteristics will make the vibration of shells in the turning-point frequency range different from that outside this range.

The order-of-magnitude relations for the singular membrane solution (denoted by the subscripts $5m$) of the membrane system outside the turning-point region and the analytic one in the whole region $a \leqslant s \leqslant b$ are (see Eq. (2))

$$
u, w, \beta, N, M, Q = \mathrm{O}(\varepsilon^{1/2}). \tag{11}
$$

And those for the pure bending solution outside the turning-point region are obtained from (10) to be

$$
u, N = \mathrm{O}(\varepsilon), \quad w = \mathrm{O}(1), \quad \beta = \mathrm{O}(\varepsilon^{-1}), \quad M = \mathrm{O}(\varepsilon^{-2}), \quad Q = \mathrm{O}(\varepsilon^{-3}). \tag{12}
$$

In addition, the order-of-magnitude relations for the five solutions (except the membrane solution) in the turning-point region can be found to be by examining (3), (4) and (8)

$$u, N = \mu^{-3/8}\mathrm{O}(\mu), w = \mu^{-3/8}\mathrm{O}(1), \quad \beta = \mu^{-3/8}\mathrm{O}(\mu^{-1}), \quad M = \mu^{-3/8}\mathrm{O}(\mu^{-2}), \quad Q = \mu^{-3/8}\mathrm{O}(\mu^{-3}). \tag{13}$$

These order-of-magnitude relations will be used in determining the natural frequencies and modes. When the ends of the shells are located in the turning-point region, the accuracy of the frequency equations and modes following obtained is $\mathrm{O}(\mu)$, otherwise it will be $\mathrm{O}(\varepsilon)$.

At either edge of the truncated shell, $s = b$ or $s = a$, three boundary conditions may be imposed. We shall restrict ourselves to consideration of the following eight cases at each edge:

$$(w\beta u), (w\beta N), (wMu), (wMN), (Q\beta u), (Q\beta N), (QMu), (QMN).$$

Here, $(w\beta u)$ represents $w = \beta = u = 0$, and so on, hence there are 64 combinations. The forms of the resulting natural frequencies and modes for the 32 edge conditions involving $Q = 0$ at $s = b$ are nearly the same and they are similar for the other 32 conditions involving $w = 0$ at $s = b$, meanwhile, the conditions involving $w = 0$ or $Q = 0$ at $s = a$ will affect a little on the modes. We shall therefore give only two derivations, one for the free–clamped edges $(QMN)_b$ and $(w\beta u)_a$ typing the first group, and the other for the clamped–free edges $(w\beta u)_b$ and $(QMN)_a$ typing the second group, where the quantities with subscripts a or b now and hereafter denote their values at $s = a$ or $s = b$, respectively. The results for the remaining 62 cases will be presented directly or discussed but not derived.

For the case of $(QMN)_b$ and $(w\beta u)_a$, if the last one or two frequencies in the turning-point range are not taken into account, this implies that the edge $s = a$ is always outside the turning-point region, then the boundary conditions at $s = a$ yield

$$\begin{aligned} &A_1\beta_{1a} + A_2\beta_{2a} = 0, \\ &A_5u_{5ma} + A_6u_{6a} = 0, \\ &A_1w_{1a} + A_2w_{2a} + A_5w_{5ma} + A_6w_{6a} = 0. \end{aligned} \tag{14}$$

Substituting (10) into (14), A_1, A_2 and A_6 can be solved and denoted by A_5

$$\begin{aligned} A_1 &= -A_5\sqrt{2}\mathrm{e}^{-\eta_a}\sin(\eta_a - \pi/8)(w_{5ma} - w_{6a}u_{5ma}/u_{6a})/H_{wa}, \\ A_2 &= -A_5\sqrt{2}\mathrm{e}^{-\eta_a}\cos(\eta_a - \pi/8)(w_{5ma} - w_{6a}u_{5ma}/u_{6a})/H_{wa}, \\ A_6 &= -A_5u_{5ma}/u_{6a}. \end{aligned} \tag{15}$$

Neglecting the exponentially small terms, the boundary conditions at $s = b$ yield

$$\begin{bmatrix} Q_{3b} & Q_{4b} & Q_{5b} \\ M_{3b} & M_{4b} & M_{5b} \\ N_{3b} & N_{4b} & N_{5b} - N_{6b}u_{5ma}/u_{6a} \end{bmatrix} \begin{bmatrix} A_3 \\ A_4 \\ A_5 \end{bmatrix} = \begin{bmatrix} 0 \\ 0 \\ 0 \end{bmatrix}. \tag{16}$$

The uniformly valid frequency equation can be obtained by inserting (3) and (8) into (16) and letting the coefficient determinant of A_3, A_4 and A_5 be zero. The results are given by, after a little manipulation,

$$\begin{vmatrix} Z_{3b}(-3) & Z_{4b}(-3) & R_b(-3) \\ Z_{3b}(-2) & Z_{4b}(-2) & R_b(-2) \\ \dfrac{C_{Nb}}{N_{6b}}Z_{3b}(2) & -Z_{4b}(2) & \zeta_b\left(\dfrac{N_{5mb}}{N_{6b}} - \dfrac{u_{5ma}}{u_{6a}} - \ln\zeta_b - \gamma + 1\right) - R_b(2) \end{vmatrix} = 0. \tag{17}$$

The first two equations of (16) lead to

$$\frac{A_3}{A_5}=\frac{Q_{4b}M_{5b}-Q_{5b}M_{4b}}{Q_{3b}M_{4b}-Q_{4b}M_{3b}}=-\frac{Z_{4b}(-3)R_b(-2)-R_b(-3)Z_{4b}(-2)}{Z_{4b}(-3)Z_{3b}(-2)-Z_{3b}(-3)Z_{4b}(-2)},$$
$$\frac{A_4}{A_5}=\frac{Q_{5b}M_{3b}-Q_{3b}M_{5b}}{Q_{3b}M_{4b}-Q_{4b}M_{3b}}=-\frac{R_b(-3)Z_{3b}(-2)-Z_{3b}(-3)R_b(-2)}{Z_{4b}(-3)Z_{3b}(-2)-Z_{3b}(-3)Z_{4b}(-2)}. \tag{18}$$

Substituting (18) and (15) into (9) yields the associated uniformly valid mode shape

$$\begin{aligned}\frac{w(s)}{A_5}=&-\sqrt{2}(w_{5ma}-w_{6a}u_{5ma}/u_{6a})\mathrm{e}^{\eta-\eta_a}\cos(\eta-\eta_a+\pi/4)\\&-\frac{Z_{4b}(-3)R_b(-2)-R_b(-3)Z_{4b}(-2)}{Z_{4b}(-3)Z_{3b}(-2)-Z_{3b}(-3)Z_{4b}(-2)}\gamma_0 Z_3(0)\\&-\frac{R_b(-3)Z_{3b}(-2)-Z_{3b}(-3)R_b(-2)}{Z_{4b}(-3)Z_{3b}(-2)-Z_{3b}(-3)Z_{4b}(-2)}[\gamma_0 Z_4(0)-w_6 Z_4(1)]\\&+\{w_{5m}-w_6[R(\zeta,1)+\ln|\zeta|+\gamma]+\gamma_0\zeta^{-1}R(\zeta,-4)\}-u_{5ma}/u_{6a}w_6\end{aligned} \tag{19}$$

and

$$\begin{aligned}\frac{u(s)}{A_5}=&-\frac{Z_{4b}(-3)R_b(-2)-R_b(-3)Z_{4b}(-2)}{Z_{4b}(-3)Z_{3b}(-2)-Z_{3b}(-3)Z_{4b}(-2)}\mu\alpha_1 Z_3(1)\\&-\frac{R_b(-3)Z_{3b}(-2)-Z_{3b}(-3)R_b(-2)}{Z_{4b}(-3)Z_{3b}(-2)-Z_{3b}(-3)Z_{4b}(-2)}[\mu\alpha_1\zeta^{-1}Z_4(-3)-u_6\zeta^{-1}Z_4(2)]\\&+\{u_{5m}-u_6[\zeta^{-1}R(2)+\ln|\zeta|+\gamma-1]+\mu\alpha_1\zeta^{-1}R(-3)\}-u_{5ma}/u_{6a}u_6.\end{aligned} \tag{20}$$

The turning point shifts from b to a as the frequency increases. Therefore after first few natural frequencies, the edge $s=b$ is away from the turning-point region and the asymptotical representations of generalized related functions may be applied. Substituting (6) and (7) into (17), (19) and (20) reduces the frequency equation and the associated mode to the form

$$\tan\theta_b\left(\frac{N_{5mb}}{N_{6b}}-\frac{u_{5ma}}{u_{6a}}\right)=-\pi, \tag{21}$$

$$\begin{aligned}\frac{w(s)}{A_5}=&-\sqrt{2}(w_{5ma}-w_{6a}u_{5ma}/u_{6a})\mathrm{e}^{\eta-\eta_a}\cos(\eta-\eta_a+\pi/4)-\frac{\pi\mathrm{e}^{-\theta_b}}{\sqrt{2}\sin\theta_b}\gamma_0 Z_3(0)\\&-\pi\cot\theta_b[\gamma_0 Z_4(0)-w_6 Z_4(1)]+\{w_{5m}-w_6[R(\zeta,1)+\ln|\zeta|+\gamma]+\gamma_0\zeta^{-1}R(\zeta,-4)\}-u_{5ma}/u_{6a}w_6,\\\frac{u(s)}{A_5}=&-\frac{\pi\mathrm{e}^{-\theta_b}}{\sqrt{2}\sin\theta_b}\mu\alpha_1 Z_3(1)-\pi\cot\theta_b[\mu\alpha_1\zeta^{-1}Z_4(-3)-u_6\zeta^{-1}Z_4(2)]\\&+\{u_{5m}-u_6[\zeta^{-1}R(2)+\ln|\zeta|+\gamma-1]+\mu\alpha_1\zeta^{-1}R(-3)\}-u_{5ma}/u_{6a}u_6.\end{aligned} \tag{22}$$

With the aid of (6) and (7), the modes outside the turning-point region can be simply expressed as

$$\begin{aligned}
&\text{as } s_* < s \leqslant b:\\
&\frac{w(s)}{A_5} = -\frac{\pi H_w(s)}{\sin\theta_b}\left[\frac{\mathrm{e}^{\theta-\theta_b}}{\sqrt{2}} + \sin(\theta-\theta_b+\pi/4)\right] + w_{5m} - \frac{N_{5mb}}{N_{6b}}w_6,\\
&\frac{u(s)}{A_5} = -\frac{\varepsilon\pi H_u(s)}{\sin\theta_b}\left[\frac{\mathrm{e}^{\theta-\theta_b}}{\sqrt{2}} - \cos(\theta-\theta_b+\pi/4)\right] + u_{5m} - \frac{N_{5mb}}{N_{6b}}u_6,\\
&\text{as } a \leqslant s < s_*:\\
&\frac{w(s)}{A_5} = -\sqrt{2}\left(w_{5ma} - \frac{u_{5ma}}{u_{6a}}w_{6a}\right)\mathrm{e}^{\eta-\eta_a}\cos(\eta-\eta_a+\pi/4) + w_{5m} - \frac{u_{5ma}}{u_{6a}}w_6,\\
&\frac{u(s)}{A_5} = u_{5m} - \frac{u_{5ma}}{u_{6a}}u_6.
\end{aligned} \tag{23}$$

For the case of $(w\beta u)_b$ and $(QMN)_a$, we shall sketch the derivation only briefly. The boundary condition equations at $s=a$ now become

$$\begin{aligned}
&A_1Q_{1a} + A_2Q_{2a} = 0,\\
&A_5M_{1a} + A_6M_{2a} = 0.\\
&A_1N_{1a} + A_2N_{2a} + A_5N_{5ma} + A_6N_{6a} = 0,
\end{aligned} \tag{24}$$

so

$$A_1 = 0, \quad A_2 = 0, \quad A_6 = -N_{5a}/N_{6a}A_6. \tag{25}$$

The boundary condition equations at $s=b$ become

$$\begin{bmatrix} \beta_{3b} & \beta_{4b} & \beta_{5b}\\ w_{3b} & w_{4b} & w_{5b} - w_{6b}N_{5ma}/N_{6a}\\ u_{3b} & u_{4b} & u_{5b} - u_{6b}N_{5ma}/N_{6a}\end{bmatrix}\begin{bmatrix} A_3\\ A_4\\ A_5\end{bmatrix} = \begin{bmatrix} 0\\ 0\\ 0\end{bmatrix}. \tag{26}$$

The uniformly valid frequency equation and associated modes are obtained with the aid of (3) and (8)

$$\begin{vmatrix} \beta_{3b} & \beta_{4b} & \beta_{5b}\\ w_{3b} & w_{4b} & w_{5b} - w_{6b}N_{5ma}/N_{6a}\\ u_{3b} & u_{4b} & u_{5b} - u_{6b}N_{5ma}/N_{6a}\end{vmatrix} = 0 \tag{27}$$

and

$$\begin{aligned}
\frac{w(s)}{A_5} =& \frac{\beta_{4b}(w_{5b} - w_{6b}N_{5ma}/N_{6a}) - \beta_{5b}w_{4b}}{\beta_{3b}w_{4b} - \beta_{4b}w_{3b}}\gamma_0 Z_3(0)\\
&+ \frac{\beta_{5b}w_{4b} - \beta_{3b}(w_{5b} - w_{6b}N_{5ma}/N_{6a})}{\beta_{3b}w_{4b} - \beta_{4b}w_{3b}}[\gamma_0 Z_4(0) - w_6 Z_4(1)]\\
&+ \{w_{5m} - w_6[R(1) + \ln|\zeta| + \gamma] + \gamma_0\zeta^{-1}R(-4)\} - N_{5ma}/N_{6a}w_6,\\
\frac{u(s)}{A_5} =& \frac{\beta_{4b}(w_{5b} - w_{6b}N_{5ma}/N_{6a}) - \beta_{5b}w_{4b}}{\beta_{3b}w_{4b} - \beta_{4b}w_{3b}}\mu\alpha_1 Z_3(\zeta,1)\\
&+ \frac{\beta_{5b}w_{4b} - \beta_{3b}(w_{5b} - w_{6b}N_{5ma}/N_{6a})}{\beta_{3b}w_{4b} - \beta_{4b}w_{3b}}[\mu\alpha_1\zeta^{-1}Z_4(-3) - u_6\zeta^{-1}Z_4(2)]\\
&+ \{u_{5m} - u_6[\zeta^{-1}R(\zeta,2) + \ln|\zeta| + \gamma - 1] + \mu\alpha_1\zeta^{-1}R(\zeta,-3)\} - N_{5ma}/N_{6a}w_6.
\end{aligned} \tag{28}$$

The reduced frequency equation and associated modes outside the turning-point region are

$$\sin(\theta_b-\pi)\left(\frac{u_{5mb}}{u_{6b}}-\frac{N_{5ma}}{N_{6a}}\right)+\pi\cos(\theta_b-\pi)-\frac{w_{5mb}-u_{5mb}/u_{6b}w_{6b}}{\sqrt{2}H_{wb}}-\frac{\varepsilon\sqrt{2}\pi H_{ub}}{u_{6b}}=0 \tag{29}$$

and

$$\begin{aligned}
&\text{as } s_*<s\leqslant b:\\
&\frac{w(s)}{A_5}=\frac{H_w(s)}{\sqrt{2}H_{wb}\sin\theta_b-w_{6b}}\left\{\left[\pi H_{wb}+T_w\cos\left(\theta_b+\frac{\pi}{4}\right)-\pi w_{6b}\sin\left(\theta_b+\frac{\pi}{4}\right)\right]e^{\theta-\theta_b}\right.\\
&\qquad\left.-\left[\sqrt{2}\pi H_{wb}\sin(\theta-\theta_b+\pi/4)+T_w\sin(\theta+\pi/4)+\pi w_{6b}\cos(\theta+\pi/4)\right]\right\}\\
&\qquad+w_{5m}-[u_{5mb}/u_{6b}+2\pi H_{wb}\varepsilon H_{ub}/u_{6b}(\sqrt{2}H_{wb}\sin\theta_b-w_{6b})^{-1}]w_6,\\
&\frac{u(s)}{A_5}=\frac{\varepsilon H_u(s)}{\sqrt{2}H_{wb}\sin\theta_b-w_{6b}}\left\{\left[\pi H_{wb}+T_w\cos\left(\theta_b+\frac{\pi}{4}\right)-\pi w_{6b}\sin\left(\theta_b+\frac{\pi}{4}\right)\right]e^{\theta-\theta_b}\right.\\
&\qquad\left.+\left[\sqrt{2}\pi H_{wb}\cos(\theta-\theta_b+\pi/4)+T_w\cos(\theta+\pi/4)-\pi w_{6b}\sin(\theta+\pi/4)\right]\right\}\\
&\qquad+u_{5m}-\left[u_{5mb}/u_{6b}+2\pi H_{wb}\varepsilon H_{ub}/u_{6b}(\sqrt{2}H_{wb}\sin\theta_b-w_{6b})^{-1}\right]u_6,\\
&\text{as } a\leqslant s<s_*:\\
&w(s)=A_5(w_{5m}-N_{5ma}/N_{6a}w_6),\quad u(s)=A_5(u_{5m}-N_{5ma}/N_{6a}u_6),
\end{aligned} \tag{30}$$

where, $T_w=w_{5mb}-w_{6b}N_{5ma}/N_{6a}$.

It should be noted that the order-of-magnitude of the last two terms on the left side of (29) is $O(\varepsilon^{1/2})$ from the order-of-magnitude relations (11). One can see a significant difference between the frequency equations (29) and (21) and modes (30) and (22) that for the present case involving $w=0$ at $s=b$ the terms of $O(\varepsilon^{1/2})$ appear in the frequency equation as well as in the mode shape. Another difference is the bending boundary layer effect at $s=a$ in the mode for w disappear for the present case involving $Q=0$ at $s=a$.

For the case of $(Q\beta N)_b$ and $(wMu)_a$, the reduced frequency equation and associated modes outside the turning-point region become

$$\tan\left(\theta_b-\frac{\pi}{4}\right)\left(\frac{N_{5mb}}{N_{6b}}-\frac{u_{5ma}}{u_{6a}}\right)=-\pi \tag{31}$$

and

$$\begin{aligned}
&\text{as } s_*<s\leqslant b:\\
&\frac{w(s)}{A_5}=\frac{\pi H_w(s)}{\cos(\theta_b+\pi/4)}\cos(\theta-\theta_b)+w_{5m}-\frac{N_{5mb}}{N_{6b}}w_6,\\
&\frac{u(s)}{A_5}=\frac{\varepsilon\pi H_u(s)}{\cos(\theta_b+\pi/4)}\sin(\theta-\theta_b)+u_{5m}-\frac{N_{5mb}}{N_{6b}}u_6,\\
&\text{as } a\leqslant s<s_*:\\
&\frac{w(s)}{A_5}=-\left(w_{5ma}-\frac{u_{5ma}}{u_{6a}}w_{6a}\right)e^{\eta-\eta_a}\cos(\eta-\eta_a)+w_{5m}-\frac{u_{5ma}}{u_{6a}}w_6,\\
&\frac{u(s)}{A_5}=u_{5m}-\frac{u_{5ma}}{u_{6a}}u_6.
\end{aligned} \tag{32}$$

Note the bending boundary layer effect at $s=b$ disappears in the mode for this case.

For the case of $(wMu)_b$ and $(Q\beta N)_a$, the corresponding reduced frequency equation and associated modes are given by

$$\sin\left(\theta_b-\frac{3\pi}{4}\right)\left(\frac{u_{5mb}}{u_{6b}}-\frac{N_{5ma}}{N_{6a}}\right)+\pi\cos\left(\theta_b-\frac{3\pi}{4}\right)-\frac{w_{5mb}-u_{5mb}/u_{6b}w_{6b}}{2H_{wb}}-\frac{\varepsilon\pi H_{ub}}{u_{6b}}=0 \tag{33}$$

and

$$\begin{aligned}
&\text{as } s_*<s\leqslant b:\\
&\frac{w(s)}{A_5}=\frac{H_w(s)}{2H_{wb}\sin(\theta_b+\pi/4)-w_{6b}}\left\{\left[\pi w_{6b}\cos\left(\theta_b+\frac{\pi}{4}\right)-T_w\sin\left(\theta_b+\frac{\pi}{4}\right)\right]e^{\theta-\theta_b}\right.\\
&\qquad\left.-[2\pi H_{wb}\sin(\theta-\theta_b)+T_w\sin(\theta+\pi/4)+\pi w_{6b}\cos(\theta+\pi/4)]\right\}\\
&\qquad+w_{5m}-\left[u_{5mb}/u_{6b}+2\pi H_{wb}\varepsilon H_{ub}/u_{6b}(2H_{wb}\sin(\theta_b+\pi/4)-w_{6b})^{-1}\right]w_6,\\
&\frac{u(s)}{A_5}=\frac{\varepsilon H_u(s)}{2H_{wb}\sin(\theta_b+\pi/4)-w_{6b}}\left\{\left[\pi w_{6b}\cos\left(\theta_b+\frac{\pi}{4}\right)-T_w\sin\left(\theta_b+\frac{\pi}{4}\right)\right]e^{\theta-\theta_b}\right.\\
&\qquad\left.+[2\pi H_{wb}\cos(\theta-\theta_b)+T_w\cos(\theta+\pi/4)-\pi w_{6b}\sin(\theta+\pi/4)]\right\}\\
&\qquad+u_{5m}-[u_{5mb}/u_{6b}+2\pi H_{wb}\varepsilon H_{ub}/u_{6b}(2H_{wb}\sin(\theta_b+\pi/4)-w_{6b})^{-1}]u_6,\\
&\text{as } a\leqslant s<s_*:\\
&w(s)=A_5(w_{5m}-N_{5ma}/N_{6a}w_6),\quad u(s)=A_5(u_{5m}-N_{5ma}/N_{6a}u_6),
\end{aligned} \tag{34}$$

where, T_w is the same as that in (30).

All the frequency equations and modes of 64 combinations of edge conditions are involved in the four forms above. We may explain this as follows: It can be seen from (3), (8) and (11) that all six solutions for u and N posses the same expressions and same order-of-magnitude, hence the alteration of the membrane boundary conditions at each edge does not change the forms of the frequency equations and modes. For example, to obtain the frequency equations and modes for the case of $(wMN)_b$ and $(Q\beta N)_a$, it suffices to replace u_{5mb}, u_{6b} with N_{5mb}, N_{6b} in the formulas (33) and (34). Another important reason is the fact that the bending boundary conditions at $s=a$ contribute nothing to the frequency equations and appear at most as boundary layer functions in the modes for w. For cases with $Q=0$ at $s=a$, the boundary layer effects disappear, and for remaining cases of $(w\beta\times)_a$ and $(wM\times)_a$, the forms of the boundary layer functions are presented in (23) and (32), where the cross $\times$ now and in this paragraph denotes u or N. Thus the eigenvibration forms for the 64 combinations of edge conditions considered can come down to four forms for cases of $(QM\times)_b$, $(Q\beta\times)_b$, $(wM\times)_b$ and $(w\beta\times)_b$ all shown above, which can be further divided into two groups, with or without terms of $O(\varepsilon^{1/2})$ corresponding to the cases involving $w=0$ or $Q=0$ at $s=b$, respectively.

4. Discussion

In Section 3 we have seen that the natural frequencies and mode shapes for various boundary conditions in the turning-point range. The following comments are relevant.

First, it can be seen that for all cases in the region $a\leqslant s<s_*$ the modes for u and w all consist of only membrane solutions of $O(\varepsilon^{1/2})$ apart from the bending boundary layer functions, if existing, and that in the region $s_*<s\leqslant b$ the modes for w involve the bending terms of $O(1)$ and membrane terms of $O(\varepsilon^{1/2})$, and for u involve the membrane terms of $O(\varepsilon^{1/2})$ and bending terms of $O(\varepsilon)$. The modes in the turning-point range will therefore exhibit two features observed by Hartung and Loden (1970), Frankort (1975) and Tao and Zhang (1998) and also shown in Fig. 3: one is that two motion types appear in the shell at the same time,

namely, the membrane motion in the region $a \leqslant s < s_*$ with the same order-of-magnitude for u and w and with a long wavelength, and the bending motion in the region $s_* < s \leqslant b$ with the transverse amplitude much higher than the longitudinal one and with a short wavelength; the other is that the shell vibrates vigorously in the region $s_* < s \leqslant b$ while it remains relatively quiescent in the region $a \leqslant s < s_*$. As the frequency increases, the turning point shifts from b to a, and the bending motion region enlarges. The features become more pronounced as the thickness of shells decreases. Somewhat unexpectedly, the order-of-magnitude relations for the degree of dominance in the modes in the turning-point range are of $O(\varepsilon^{-1/2})$, rather than $O(\varepsilon^{-1})$ in other frequency range, which, as well as the presence of turning point, comes actually from the singularity of the membrane system equations.

Second, from the frequency equations and associated modes outside the turning-point region, one can see all of them contain contributions from both bending and membrane solutions. However, above the turning-point range Ross and Matthews (1967) found two sets of natural frequencies, in which, the one involves only membrane solutions, and the other involves only bending solutions, hence the names the membrane frequency and the bending frequency. He also pointed out that at least the modes for w associated with the bending frequencies and the modes for u associated with the membrane frequencies are wholly of bending type and membrane type, respectively. Further he proved below the turning-point range the bending type modes cannot occur. We may therefore conclude that the coactions of the bending and membrane solutions characterize the vibration of shells in the turning-point range. It should be noted that the coupling feature results directly from the symmetric coupling structure of the solutions mentioned in the introduction and in the observation of (10): from (10) one can see in traversing the turning-point region the singular membrane solution gives birth to the second bending solution with a coupling coefficient π and the fourth bending solution gives birth to the analytic membrane solution with a coupling coefficient -1, while the coefficient $-\pi$ appearing in the frequency equations is just the product of the two coupling coefficients. Clearly as long as one of the coupling coefficient vanishes, the frequency Eqs. (21), (29), (31) and (33) will separate into two recognizable classes: one contains only the membrane solutions obtained directly by applying the membrane solutions to the corresponding membrane boundary conditions, and the other contains contributions only from the bending solutions. So the coupling vibration in this frequency range depends on the symmetric coupling structure of the solutions. The turning point is physically interpreted as the site of localized interaction between the bending and stretching effects Ross (1966). However, the effect of the turning point is global, rather than only limited to the turning-point region. Even when it shifts far away from the edge, the turning point still exerts a profound influence on the behavior of nature frequencies and modes.

The conclusion of the coupling of bending and membrane solutions for frequencies and modes can be reinforced by examination of the resonance phenomena for stretching energy V_S and bending energy V_B of a conical shell with both ends freely supported subject to a longitudinal force at the small end of the shell, and the results are obtained from the finite element method (FEM) and shown in Fig. 1. (The parameters of the cone are given in the next section, and the finite element model and program used in this paper are described by Zienkiewicz (1971) and Zhang (1993), for which the element is an axisymmetric conical ring element with six degrees of freedom, and the cone is divided into 50 conical ring elements in calculation.) One can see from Fig. 1 that at each resonant frequency V_S and V_B reach their peaks simultaneously, while there are no evident peaks and dips for the ratio of V_B to V_S. It is well known that only membrane resonance would occur for uncoupled bending and membrane solutions under this sort of boundary conditions.

The term of bending resonant frequency is often used in the turning-point range in the investigation of loudspeaker cones by Frankort (1975), Tao and Zhang (1998) and Zhang and Tao (2001). However, it appears to be improper in view of the coupling of bending and membrane solutions for the frequency equation, and the term "coupling resonant frequency" may be properly applied.

Third, the fact of the coupling of bending and membrane solutions for frequencies and modes in the turning-point range implies that the shallow shell theory is not applicable in this frequency range, because

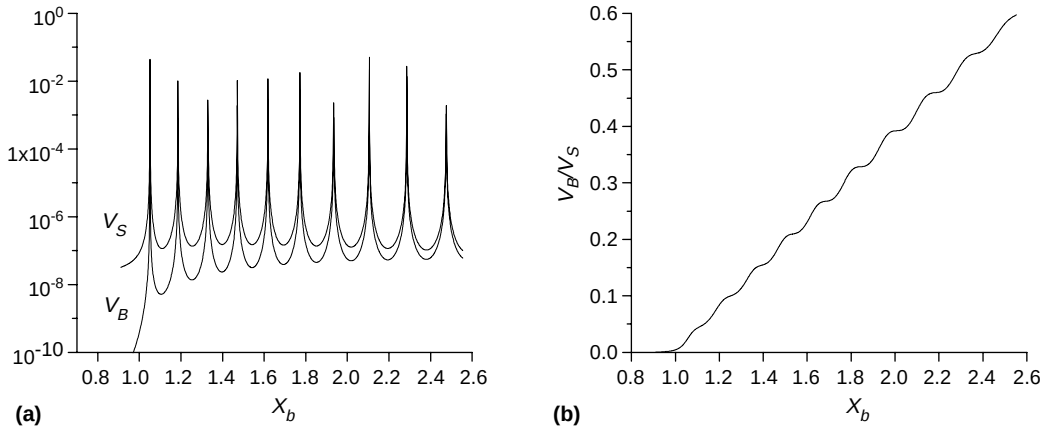

Fig. 1. First ten resonance phenomena for stretching energy V_S and bending energy V_B of the cone with free–free boundary conditions driven by a longitudinal force at small end.

in the shallow shell theory the effect of the longitudinal inertia on the transverse modes is ignored, which is widely used by Tang (1964), Seide (1965), Sun (1987) and many other researchers to obtain the series solutions.

Fourth, one can also see that only the membrane boundary conditions at $s = a$ play evident part in the natural frequencies and modes in the turning-point range. This fact can interpret the phenomenon found by Hartung and Loden (1970) from numerical calculation, namely, a change of boundary conditions at the large end of the cone would have much more effect on frequencies and modes than at the small end. And the effect of bending edge conditions at $s = b$ will be formulated in the next section.

Fifth, either the frequency equations or the modes contain two membrane solutions of the membrane system, as mentioned early, which in the turning-point range usually have to be found by numerical integration on the second-order membrane equations or in a series form. Hence the present work is to reduce the problem of solving a sixth-order differential equation to solving the second-order membrane system. Even with numerical calculations available, we may expect it would contribute much to understanding numerical results and be helpful for analysis of nonlinear vibration of shells. And however, the formulas for the bending-edge-condition effect and for the frequency spacing, which contain bending terms only, will be given in the next section.

5. Application to conical shells

In this section, we shall validate the present results first, and then present the formulas for the bending-edge-condition effect and frequency spacing.

For conical shells, $s = b$ and $s = a$ then denote the large and small ends of shells, respectively. Introduce the variable transformation

$$X = \Omega R_2 = \Omega s \tan\alpha, \tag{35}$$

to simplify the expression of the phase function θ_b as

$$\theta_b = G/\sqrt{X_b}\int_1^{X_b}(1-x^{-2})^{1/4}\,\mathrm{d}x = G\Psi(X_b), \tag{36}$$

where α is the semi-vertex angle of conical shell, and $G = \frac{\sqrt{R_{2b}}}{\varepsilon \tan \alpha}$ is a combination of shell geometry parameters used by Seide (1965). The turning-point range limits the value of X_b to the range $1 \leqslant X_b \leqslant R_{2b}/R_{2a}$, and the minimum and maximum values of X_b correspond to the turning points occurring at large and small ends, respectively. Therefore, we may interpret that X_b is a normalized frequency parameter with the normalizing factor being the lower limit frequency of the turning-point range of a given conical shell. And one can see that $\Psi(X_b)$ is a frequency function independent of cone geometry, $\Psi(X_b)$ and its derivative can be expressed in terms of the hypergeometric function F known as the Gauss series

$$\begin{aligned}\Psi(X_b) &= \left[F(-0.5,-0.25,0.5,x)/\sqrt{x}\right]\Big|_1^{X_b^{-2}}/\sqrt{X_b} = \sqrt{X_b}F(-0.5,-0.25,0.5,X_b^{-2}) - 1.31103/\sqrt{X_b},\\ \Phi(X_b) &= \frac{\mathrm{d}\Psi}{\mathrm{d}X_b} = \frac{1}{2\sqrt{X_b}}\left[2(1-X_b^{-2})^{1/4} - F(-0.5,-0.25,0.5,X_b^{-2}) + \frac{1.31103}{X_b}\right],\end{aligned} \tag{37}$$

where the hypergeometric function F can be closely approximated by the first two terms of its series expansion about zero, with an error of less than 1.5% for $X_b > 1.2$, as follows:

$$F(-0.5,-0.25,0.5,X_b^{-2}) = 1 + 0.25X_b^{-2}. \tag{38}$$

The calculated dependence of Ψ and Φ on X_b is shown in Fig. 2. It can be seen that except a few initial values of X_b, they are smooth functions and that they can be accurately approximated by the approximate results, obtained from after the substitution of (38) for the hypergeometric function F in (37).

Under calculation, the conical shell has a semi-vertex angle α of 50°, a ratio of small to large end radius $R_a/R_b = 0.20482$, and the dimensionless thickness parameter $\varepsilon/\sqrt{R_b} = 0.02896$, so the geometry parameter $G = 36.142$, which has been taken as a typical example for loudspeaker cone investigated in detail in Frankort (1975). The first five values of frequency parameter X_b and the corresponding θ_b/π are calculated and shown in Table 1 by the present formulas and the Finite Element Method. The pure membrane solutions appearing in the formulas are obtained numerically from the second-order membrane equations. It can be seen that the two results are nearly the same. Modes obtained from the two methods are shown in Fig. 3, and seen that they also exhibit an almost complete agreement. As pointed out by Zhang and Zhang (1991), the solutions of the present form satisfy the accuracy of thin shell theory.

Two conclusions can be obtained from Table 1. First, the effect of relaxing the edge conditions is, of course, a reduction of the natural frequencies. One can see that the values of θ_{bn} for the same values of n increase by nearly $\pi/4$, $\pi/2$ and $\pi/4$ from the first case to the fourth case in turn, except the first one or two frequencies for which the turning points lie in the immediate vicinity of the large end of the shell

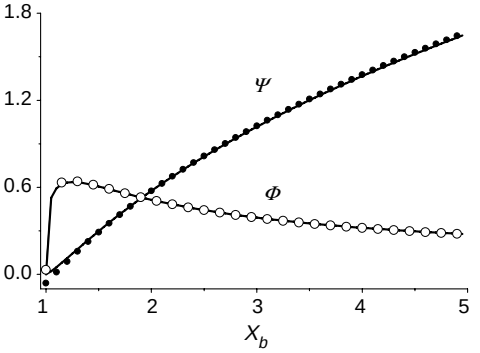

Fig. 2. Dependence of frequency function Ψ and its derivative Φ on frequency parameter X_b: (—) exact results, (●) approximate result for Ψ, (○) approximate result for Φ.

Table 1
The first five values of frequency parameter X_b and corresponding θ_b/π from two methods

Edge conditions	Calculation methods	X_{b1}, θ_{b1}/π	X_{b2}, θ_{b2}/π	X_{b3}, θ_{b3}/π	X_{b4}, θ_{b4}/π	X_{b5}, θ_{b5}/π
$(QMN)_b$ $(w\beta u)_a$	Present	1.073	1.224	1.371	1.517	1.668
	Formulas	0.39	1.45	2.51	3.54	4.56
	FEM	1.075	1.224	1.370	1.515	1.667
$(Q\beta N)_b$ $(wMu)_a$	Present	1.106	1.265	1.406	1.555	1.707
	Formulas	0.62	1.75	2.77	3.80	4.81
	FEM	1.108	1.265	1.406	1.553	1.705
$(wMN)_b$ $(Q\beta u)_a$	Present	1.202	1.327	1.486	1.625	1.791
	Formulas	1.29	2.20	3.33	4.27	5.35
	FEM	1.202	1.327	1.485	1.624	1.788
$(w\beta N)_b$ $(QMu)_a$	Present	1.246	1.358	1.525	1.661	1.833
	Formulas	1.61	2.43	3.60	4.51	5.61
	FEM	1.246	1.359	1.525	1.660	1.831

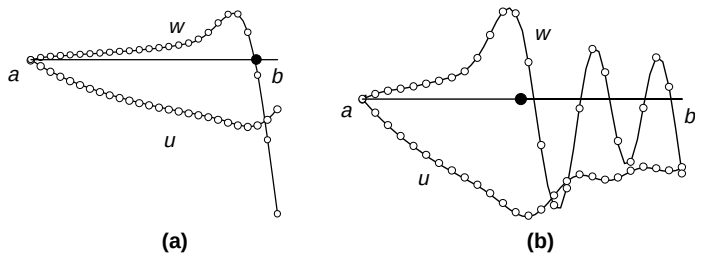

Fig. 3. Longitudinal displacement u and transverse displacement w modes with u magnified 10× at (a) the first frequency, (b) the fifth frequency: (—) present results, (▲) results from FEM, (●) position of turning point.

and therefore the reduced frequency equations are not applicable ($\zeta_b > 5$, the condition to use the asymptotic representations of the generalized related functions, corresponds to $\theta_b > 1.9\pi$). This fact could be expected from the reduced frequency Eqs. (21), (31), (33) and (29) by observing that the initial phases of the bending terms lag behind by $\pi/4$, $3\pi/4$ and π in turn in these formulas and that the four cases in Table 1 have the same membrane edge conditions. Since the membrane solutions are slowly varying functions for the position and therefore for the frequency while the bending terms are rapidly varying ones, the membrane solutions can be approximately regard as constants for $\theta_b \to \theta_b + \pi$. Accounting for Q, M and β are respectively the third, second and first order of derivatives for w for bending solutions, the formula for the effect of bending-edge-conditions at $s = b$ with the same membrane edge conditions can then be given by

$$\theta_{bn(\times\times\times)_b} = \theta_{bn(w\beta\times)_b} - (j-1)\pi/4, \tag{39}$$

where j is the sum of the derivative order for w of the two bending quantities appearing in the edge conditions at $s = b$, and the cross '×' denotes any proper variable.

Second, it can be seen that for each case the spacing of phase function θ_b is about π when the turning point shifts away from the edge vicinity. This phenomenon can be interpreted by almost the same reason. Hence the frequency spacing formula can be written in the form

$$\theta_{bn+1} - \theta_{bn} = \pi. \tag{40}$$

With the aid of Taylor's Series, the formula (40) can be approximately rewritten in an explicit form

$$X_{bn+1} - X_{bn} = \frac{\theta_{bn+1} - \theta_{bn}}{G\Phi(X_{bn})} = \frac{\pi}{G\Phi(X_{bn})}. \tag{41}$$

It can be shown that the frequency spacing depends mainly on the shell geometry combination G and increases with increasing wall thickness and semi-vertex. Also one can see it is uneven for n, becoming somewhat larger for increasing n. The accuracy of (41) would be expected to increase with increasing G, since for large value of G the frequency spacing is so small that the difference between $\Phi(X_{bn})$ and $\Phi(X_{bn+1})$ can be negligible. Eq. (39) also possesses an explicit expression analogous to (41).

Eqs. (39) and (40) are also applicable to general revolution shells because the fast variation for the bending solutions and slow variation for the membrane solutions is characteristic of any thin shell, whether conical or not, since Eqs. (39) and (40) result directly from this characteristic.

The validation of Eqs. (40) and (41) is made for cones with free–clamped edge condition and the results are shown in Fig. 4. It indicates that the results quite agree with 1 except first two spacings and three regions in Fig. 4a for $\alpha = 19.5842°$, and that Eq. (40) can be accurately approximated by Eq. (41), with the agreement becoming, as expected, increasingly better for increasing G. The exceptional regions appear in somewhat periodic way. Calculations show that in each of these regions two membrane characteristic frequencies occur: one where $N_{6b} = 0$, in the neighborhood of which the frequency equation obtained from (21) is given by $\theta_{bn} \approx n\pi$; the other where $N_{5mb}u_{6a} = N_{6b}u_{5ma}$, in the neighborhood of which frequency Eq. (21) becomes $\theta_{bm} \approx m\pi + \pi/2$. Obviously, the more closely the two membrane characteristic frequencies are spaced, the

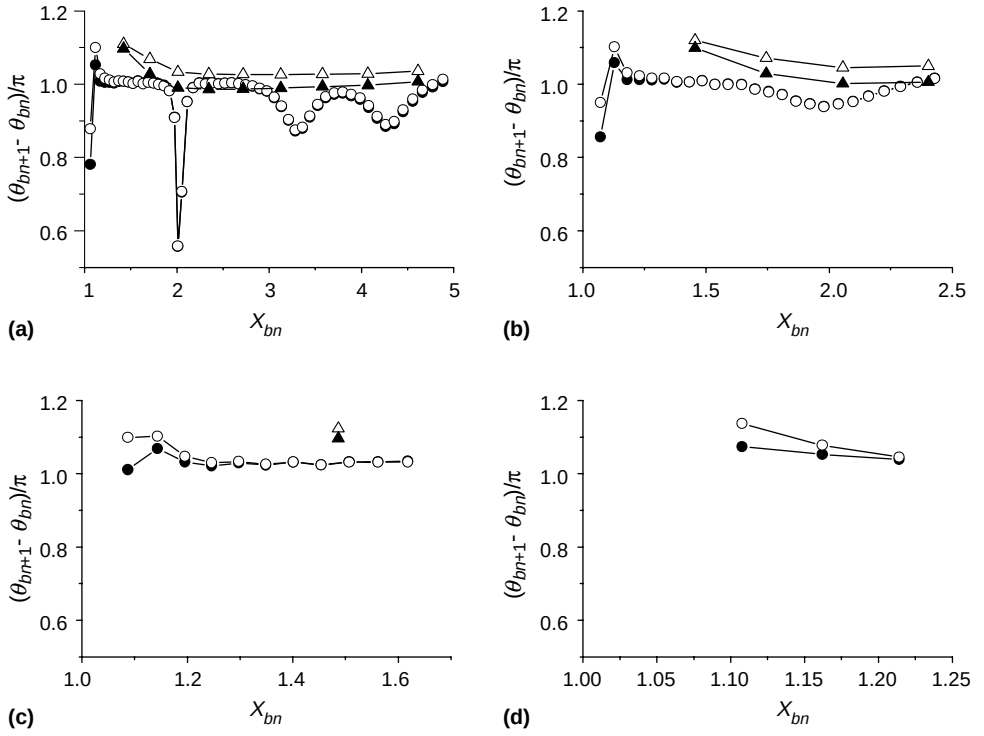

Fig. 4. Spacings of phase function θ_b/π versus frequency parameter X_b for $\varepsilon/\sqrt{R_b} = 0.02896$ and (a) $R_a/R_b = 0.2$, (b) $R_a/R_b = 0.4$, (c) $R_a/R_b = 0.6$, (d) $R_a/R_b = 0.8$: (–●–) $G = 100$, $\alpha = 19.5842°$, exact results; (–○–) $G = 100$, $\alpha = 19.5842°$ results of Eq. (41); (–△–) $G = 20$, $\alpha = 72.2808°$, exact results ; (–▲–) $G = 20$, $\alpha = 72.2808°$, results of Eq. (41).

more evident the error for the frequency spacing Eq. (40). The extreme case $\theta_{bn+1} - \theta_{bn} = \pi/2$ happens to occur in the first exceptional region. Note the second membrane characteristic frequency equation can be actually obtained by applying the membrane solutions to the membrane edge conditions, so the resulting frequencies are the membrane natural frequencies predicted by the membrane systems. The exceptional region does not occur for other cases for which the slant lengths of the cones are too short for the membrane frequencies predicted by the membrane systems to occur.

In conclusion, we may think from the results that the formula (39) for the effect of bending edge conditions and frequency spacing formula (40) are applied with exceptional cases for which the membrane frequencies predicted by the membrane systems occur, and that for short shells with the first natural frequency predicted by the membrane theory above the turning-point range, the results can be applied without exception.

Acknowledgement

The work is supported by Shanghai Leading Academic Discipline Project (Y0103) and Zhejiang Provincial Natural Science Foundation of China (Y104574).

References

Frankort, F.J.M., 1975. Vibration and Sound Radiation of Loudspeaker Cones. N. V. Philips' Gloeilampenfabrieken, Eindhoven.

Gol'denveizer, A.L., 1980. Free vibration spectrum structure of a shell of revolution. In: Nemat-Nasser, S. (Ed.), Mechanics Today. Pergamon Press, Oxford, pp. 67–82.

Gol'denveizer, A.L., Lidskiy, V.B., Tovstic, P.E., 1979. Free Vibration of Thin Elastic Shells (in Russian). Nauka, Moscow.

Hartung, R.F., Loden, W.A., 1970. Axisymmetric vibration of conical shells. Journal of Spacecraft and Rockets 7, 1153–1159.

Ross Jr., E.W., 1966. Transition solutions for axisymmetric shell vibrations. Journal of Mathematical Physics 54, 335–355.

Ross Jr., E.W., Matthews, W.T., 1967. Frequencies and mode shapes for axisymmetric vibration of shells. Journal of Applied Mechanics 34, 73–80.

Seide, P., 1965. On the free vibrations of simply supported truncated conical shells. Israel Journal of Technology 3, 50–61.

Steele, C.R., 1976. Application of the WKB method in solid mechanics. In: Nemat-Nasser, S. (Ed.), Mechanics Today. Pergamon Press, Oxford, pp. 243–295.

Sun, B.H., 1987. Exact solution of eigenfrequencies of conical shells (in Chinese). Acta Mechanica Sinica 19, 136–145.

Tang, C.T., 1964. The vibration modes and eigenfrequencies of circular conical shells. Scientia Sinica 13, 1189.

Tao, Q.T., Zhang, Z.L., 1998. Frequency equation of thin shell vibration in the transition range. Journal of Sound and Vibration 217, 33–41.

Zhang, R.J., 1988. Asymptotic solutions to the equations of free vibrations of thin shells of revolution (in Chinese), Ph.D. Thesis. Tsinghua University, Beijing.

Zhang, Z.L., 1993. The variational Young's moduius problem of loudspeaker vibrations (in Chinese), M.S. Thesis. Nanjing University, Nanjing.

Zhang, Z.L., Tao, Q.T., 2001. Experimental study of non-linear vibrations in a loudspeaker cone. Journal of Sound and Vibration 248, 1–8. doi:10.1006/jsvi.2001.3727.

Zhang, R.J., Zhang, W., 1991. Turning point solution for thin shell vibration. International Journal of Solids and Structures 27, 1311–1326.

Zhang, Z.L., Cheng, C.J., 2005. Uniform solutions for vibration of revolution shells in turning-point range, Journal of Sound and Vibration, submitted for publication.

Zienkiewicz, O.C., 1971. The Finite Element Method in Engineering Science. McGraw-Hill, London.